ADVANCED MATERIALS INTERFACES
www.advmatinterfaces.de

The Thermal Oxidation of TiAlN High Power Pulsed Magnetron Sputtering Hard Coatings as Revealed by Combined Ion and Electron Spectroscopy

*Martin Wiesing, Teresa de los Arcos, and Guido Grundmeier**

The thermal oxidation of TiAlN hard coatings deposited by High Power Pulsed Magnetron Sputtering (HPPMS) is investigated at room temperature and 800 K at oxygen pressures ranging from 10^{-6} to 10^{-2} Pa by means of in situ X-ray and Ultraviolet Photoelectron Spectroscopy as well as Low Energy Ion Scattering. The spectra reveal that oxygen binds selectively to titanium during the initial chemisorption step and simultaneously some oxygen is dissolved into subsurface layers, which stay metallic. Enhanced oxidation results into continuous formation of a multilayered oxide film including oxynitride TiAl(O,N) as a metastable reaction product buried below an oxidic top layer. This top layer is either composed of mixed TiAlO after oxidation at 800 K or of segregated TiO_2 and Al_2O_3 when oxidizing at 293 K. Additionally, evaluation of UV-valence bands reveals nitrogen doping of the surface oxide films. The results are of high relevance for tailoring of the surface characteristics of TiAlN after deposition, for the design of TiAlN multilayers and for an improved understanding of the interactions of gas particles with these coatings.

1. Introduction

Ternary hard coatings such as TiAlN have found widespread use for cutting tools due to their high hardness and resistance against wear and thermal oxidation.[1,2]

Early studies of high temperature oxidation of TiAlN revealed the surface enrichment of aluminum and thus the formation of a protective Al_2O_3 cover layer on top of titanium nitride and oxynitride.[2] This near surface structure clarified the improved oxidation resistance of TiAlN when compared to the prototypic TiN. Notably, investigations on the effect of the aluminum content on the oxidation resistance revealed that the formation of a closed Al_2O_3 cover layer was deteriorated at higher aluminum concentrations due to the formation of a mixed Al–Ti oxide and decomposition of the metastable cubic phase of TiAlN.[3,4] Recently, such hard coatings have attracted additional interest due to the observed low wettability of polymers on surfaces of TiAlN and TiAl(O,N), which makes these coatings promising candidates as functional coatings of tools used in polymer injection molding.[5] In this case the TiAlN coating is in contact with an oxygen containing polymer melt at a temperature of 500–700 K. Among the plethora of parameters that govern the development of specific surface-near multilayer structures upon oxidation the stoichiometry and internal structure of the coating previous to oxidation is of central importance. These latter aspects can be tailored up to a certain point through control of the deposition process. In particular, high power pulsed magnetron sputtering (HPPMS) has gained much attraction recently for the deposition of hard coatings with high density and improved properties in terms of adhesion, hardness, and low surface roughness.[6–9] The reason for the increased quality of HPPMS-deposited films lies in the highly increased fraction of ionized species during deposition, which allows for a higher degree control on the growing film structure.[9]

However, independently of the degree of control achievable during the deposition process, a final issue critical for the establishment of a top oxide layer is the way samples react to different ambient conditions once the deposition process is finished. This aspect has been explored both theoretically and experimentally. Music et al., for example, used ab initio molecular dynamics to investigate the interaction of TiAlN surfaces with residual and environmental gases, namely O_2, H_2O, and CO_2.[10] Greczynski et al. showed experimentally how the surface composition of TiN films dramatically changed as function of the conditions in which the venting procedure is performed.[11] In short, in order to achieve specific oxide-terminated surfaces, the basic mechanisms by which thermal oxidation proceeds in the medium temperature range need to be better understood.

Preliminary experimental investigations of the oxygen chemisorption layer of HPPMS-deposited TiAlN have been already performed, showing that the oxygen chemisorption is self-limited and results into a surface segregated Ti_2O_3 layer.[12] However, the present work is intended to provide a more accurate microscopic model of the chemisorption layer by using combined in situ X-ray Photoelectron Spectroscopy (XPS) and Low Energy Ion Scattering (LEIS). Based on the results obtained, a microscopic model of the oxidation of TiAlN at medium temperatures which are relevant for polymer processing will be developed.

M. Wiesing, Dr. T. de los Arcos, Prof. G. Grundmeier
Technical and Macromolecular Chemistry
University of Paderborn
Warburger Straße 100, 33098 Paderborn, Germany
E-mail: guido.grundmeier@tc.uni-paderborn.de

DOI: 10.1002/admi.201600861

2. Results and Discussion

2.1. Oxidation at 1 × 10^{-6} Pa O_2 and Room Temperature

Before surface oxidation, the TiAlN sample was cleaned from organic contaminations and its native oxide by means of Ar^+ sputter cleaning. The sputtering process is well known to affect structure and composition of the near-surface region due to preferential sputtering, atomic mixing and implantation of Ar, just to name a few.[13] It must be thereby noted, that care has to be taken when comparing the results presented with the oxidation process of hard coatings as encountered directly after deposition.

However, the samples were exposed to oxygen at a pressure of 1 × 10^{-6} Pa after sputter cleaning. The exposure time was 10 min, thus ensuring that the surface concentration of chemisorbed oxygen reached a steady value. According to Kunze et al. it is expected that the first monolayer of chemisorbed oxygen hampers the 3D growth of the oxide film at these values of oxygen pressure and substrate temperature.[12] The layer of chemisorbed oxygen was subsequently investigated in situ by XPS and LEIS.

Figure 1 shows the high resolution XPS spectra of the Ti2p, O1s, N1s, and Al2p core levels after (a) sputtering, (b) chemisorption, and (c) after LEIS characterization.

After Ar^+ sputtering (Figure 1a), the Ti2p line shape can be roughly described by two major components at binding energies of 455.0 and 456.6 eV, which are accompanied by a weaker satellite structure at 458.2 eV. The spin-orbit splitting of the

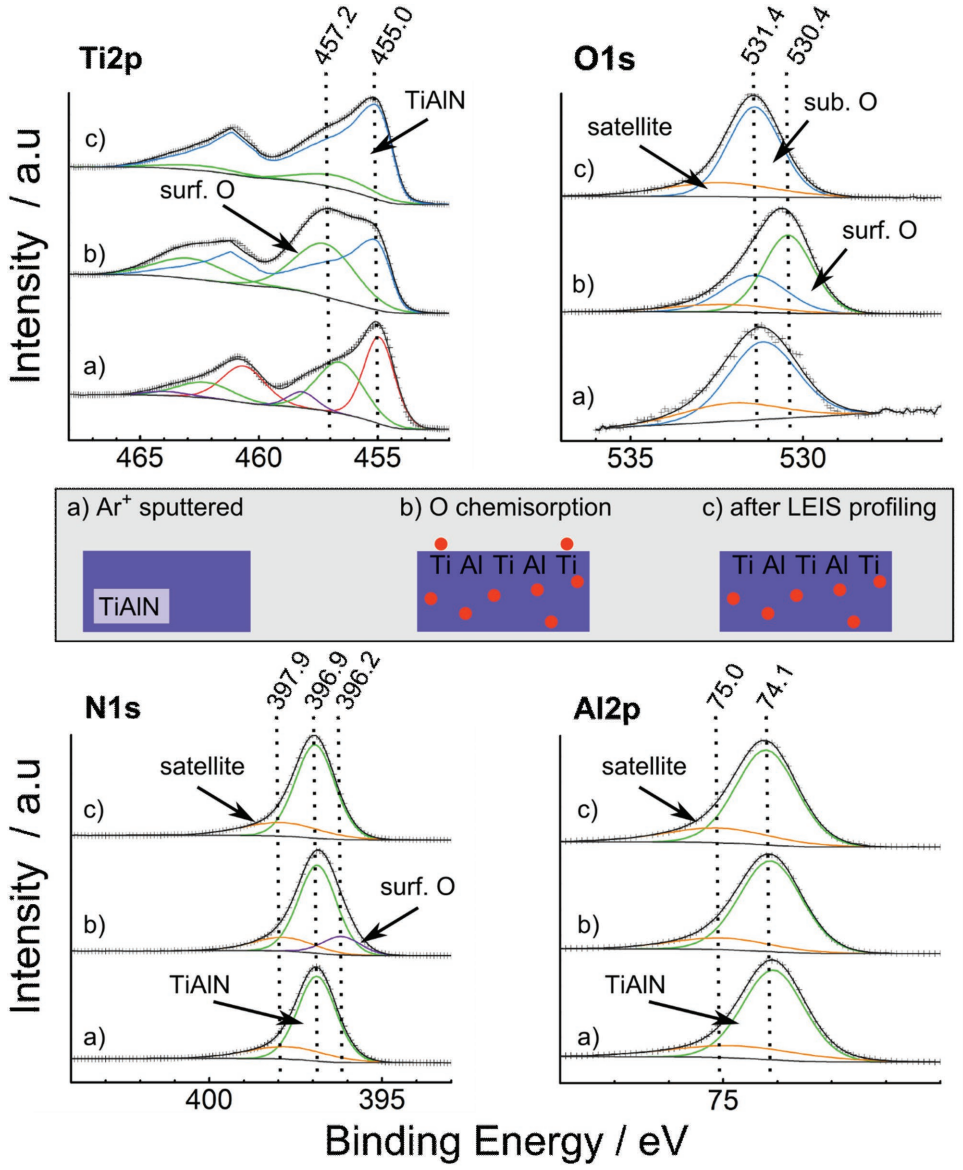

Figure 1. High-resolution XPS spectra of the Ti2p, O1s, N1s, and Al2p core levels a) after Ar^+ sputter cleaning, b) after oxygen chemisorption (10^{-6} Pa oxygen) at room temperature, and c) after measuring LEIS depth profiles of the state described in panel (b). The spectra have been normalized and shifted vertically for better visualization and the raw data are represented by symbols (+). The sketch illustrates the corresponding surface layer model for each experimental condition.

components was set to 5.7 eV for the peak fitting procedure.[14] The component at 455.0 eV was included in order to account for the presence of a well screened peak in the spectrum of TiAlN, where relaxation occurs due to transfer of a d-band electron into a locally pulled-down d-state during the photoemission process.[15–17] Complementary, the component at 456.6 eV was included for the case where no such relaxation proceeds (poorly screened peak). The satellite structure at 458.2 eV was motivated by EELS measurements of TiAlN, which show a Ti3d t_{1g}-t_{2g} intraband shake-up at 1.55 eV relative to the main signal with a relative intensity of 0.19. The satellite component in the Ti2p spectrum was set accordingly relative to the poorly screened peak at 456.6 eV. For illustration of the quality of the data and the fitting procedure, the reader is referred to Figure S1 (Supporting Information), which shows the data, fits, and residuals of Figure 1a in more detail and is representative for the XPS spectra discussed in the following.

The Ti2p line shape in TiN and TiAlN compounds is complex and has been the subject of several studies, which attribute the different components to different effects, such as an shake-up event due to Ti3d intraband transitions, changes in the screening ability of the conduction electrons associated with an increasing nitrogen content or structural effects.[15–17] A good overview about different aspects of Ti2p line shape interpretation can be found elsewhere.[18] Given the low concentration of oxygen detected after Ar^+ sputtering (below 2.5 at%; see **Table 1**) we assume that the contribution of possible oxides or oxynitrides to the Ti2p line shape can be considered as negligible and thus that the Ti2p line as measured after the sputter cleaning treatment represents the state of an essentially oxygen-free TiAlN surface. The measured Ti2p line shape directly after Ar^+ sputtering will be used as reference in all following mathematical decompositions as a whole in order to determine the additional components appearing as a consequence of oxygen exposure. This procedure is an empirical approach and neglects that the lineshape of the TiAlN substrate layers could change due to oxide overlayers, which is to some extent expected because the intraband transition represents an extrinsic energy loss mechanism. All components assigned in this publication using this empirical approach are thus primarily discussed based on qualitative arguments and reinforced by the use of complementing techniques such as LEIS and Wagner plot analysis. Where appropriate, quantitative stoichiometric calculations are discussed.

The corresponding N1s and Al2p core levels were located at 396.9 and 74.1 eV respectively, which is typical for TiAlN.[18–20] However, both signals showed a distinct tailing to the higher binding energy site, which was taken into account by fitting an additional satellite component shifted by 0.9 eV relative to the main signal. This tailing is common for several nitridic hard coatings but is scarcely discussed in literature.[21] Some authors assign this component to the appearance of N—O species.[22,23] However, tailing was also observed in essentially oxygen-free (4 at% oxygen) in situ XPS spectra of single crystalline Ti_2AlN and there are also indications that structural defects could be responsible for this spectral feature.[17,24] The weak O1s contribution left after the sputtering was fitted using a linear background and two components: one at 531.2 eV related to oxygen impurities and another component at 532.1 eV ascribed to the satellite as in the case of the N1s and Al2p spectra.

Table 1. Stoichiometry of the investigated samples in atomic percent as derived from XPS survey spectra measured at 60°.

Sample	X_{Al} [at%]	X_N [at%]	X_{Ti} [at%]	X_O [at%]	Al/Ti
Ar^+ sputtered	32.8	43.6	21.3	2.4	1.54
10^{-6} Pa, 10 min, 293 K	30.2	37.3	19.3	13.2	1.56
LEIS profiling	32.1	40.5	20.5	7.0	1.56
5×10^{-2} Pa, 24 h, 293 K	25.4	26.6	17.3	30.7	1.47
5×10^{-2} Pa, 24 h, 800 K	26.9	19.6	15.1	38.4	1.78

The Ti2p, N1s, Al2p, and O1s core level lines after exposure of the sample to oxygen for 10 min can be seen in Figure 1b. The changes induced in the Ti2p line shape were described by the appearance of an additional broad component at 457.2 eV, which was related to the formation of Ti—O bonds. The Al2p peak however was unaffected by chemisorption. The N1s lineshape was described by using the components of TiAlN and fixing their positions and the FWHM of the main signal. Further, a lower binding energy component at 396.2 eV was included and assigned to the presence of surface oxygen. This latter component was scarcely resolved and the position was thereby fixed relative to the main nitride component. This peak model was validated by the spectra of the more oxidized samples discussed below. The O1s line is decomposed into three components at 530.4, 531.4, and 532.3 eV. The component at 530.4 eV is assigned to the formation of Ti—O bonds of surface oxygen, while the component at 531.4 eV is associated with subsurface oxygen. The third component at 532.3 eV is as before ascribed to the satellite. The binding energies of the latter two components were taken from the O1s signal after LEIS profiling as discussed below and fixed for deconvolution. These assignments are justified by the LEIS characterization of the surface, as described in the following paragraphs.

After first performing XPS measurements of the chemisorbed layer, the sample was investigated in situ by LEIS and the results are shown in **Figure 2** (Supporting Information). The bombardment of the sample by He^+ ions during the measurement lead to a progressive sputtering of sample material with the corresponding changes in the LEIS spectrum as can be seen in the figure. Three main components can be identified in the LEIS spectrum at 756, 622, and 459 eV kinetic energy and are assigned to titanium, aluminum and oxygen respectively.[25] Trace amounts of nitrogen were observed in the form of a shoulder appearing at about 400 eV at the lower kinetic energy side of the oxygen signal. During LEIS "profiling," the titanium signal increased at the expense of the oxygen signal, whereas the aluminum signal remained constant. Since LEIS is almost entirely sensitive to the outermost atomic layer, this analysis shows that aluminum and titanium atoms are both present at the very surface. However, it was found that no aluminum oxide cover layer was formed during chemisorption, and that the chemisorbed O atoms preferentially bind to titanium. This interpretation is supported when considering the density of states of TiAlN and TiAl(O,N):[26] according to the stoichiometry of $Ti_{0.2}Al_{0.3}N_{0.5}$ (see Table 1), ≈1 electron is located in the Ti3d valence band, which is separated from the largely mixed

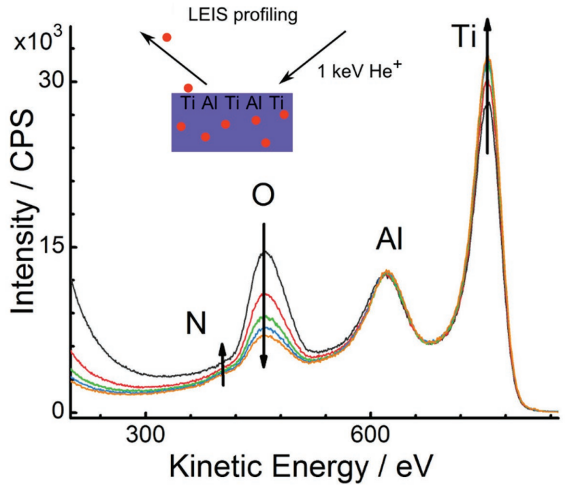

Figure 2. LEIS depth profile measured with 1 keV He^+ of the oxygen chemisorption layer on TiAlN as obtained after sputter cleaning and exposure to 10^{-6} Pa oxygen at 293 K for 10 min. Each spectrum corresponds to one scan, and all scans were performed consecutively. The arrows indicate the evolution with time.

N2p, Al3p, and O2p band by a pseudo band gap. Thus, spill-over Ti3d electrons are transferred into localized oxygen states during oxygen adsorption resulting into oxygen to bind selectively to titanium atoms at the surface. This preferential interaction of oxygen with titanium was also found within simulations of the gas/solid interactions for a TiAlN(001) surface.[10]

The LEIS characterization allows to refine the interpretation of XPS data, especially when comparing the XPS characterization of the chemisorbed layer done before (Figure 1b) and after LEIS (Figure 1c). The main effect of the LEIS measurement is the preferential sputtering of oxygen. The stoichiometry of the samples as determined from the XPS data showed that the oxygen concentration decreased to 53% of its original value, from about 13 at% after chemisorption to about 7 at% after LEIS profiling. In comparison with the oxygen LEIS signal, a larger decrease to 31% of the initial oxygen value was observed. Since the LEIS oxygen signal reflects surface oxygen atoms only, this shows that oxygen is also present in subsurface layers and is thereby measured by XPS. When comparing Figure 1b,c, the sputter removal of surface oxygen is further associated with the disappearance of the O1s component at 530.4 eV, which reinforces the interpretation that this component represents the surface oxygen atoms. In turn, the other component at 531.4 eV is consequently related to subsurface oxygen species. These assignments are qualitatively in good agreement with chemical shifts of chemisorbed oxygen on α_2-TiAl, where dissociated surface oxygen was found at 530.7 and subsurface oxygen at 532.0 eV.[27] The results show that the oxygen chemisorption on TiAlN is accompanied by inward migration of oxygen.

The oxygen behavior is also reflected in the Ti2p and N1s peaks. In the case of Ti2p, the Ti—O component at 457.2 eV diminished also to 31% of its original intensity after LEIS profiling. This matches the decrease of the LEIS oxygen signal and thus allows to assign this Ti2p component similarly to titanium binding to surface oxygen. This further implicates that one oxygen atom is bound to one titanium atom at the surface. Accordingly, the component of N1s at 396.2 eV also decreased concomitantly with the surface oxygen component of the Ti2p spectrum and is thereby similarly related to the presence of surface oxygen. This finding is in agreement with earlier observations of oxynitride at this binding energy, which show that the binding energy of nitride is affected by the presence of oxygen.[17]

The 1:1 stoichiometry of the surface oxygen layer can be supported by means of cross-peak self-consistency calculations: the amount of oxygen related only to surface oxygen (Ti—O) was calculated from both Ti2p (component at 457.2 eV) and O1s (component at 530.4 eV) spectra assuming a stoichiometry of 1:1 for the Ti—O structure.[28] The surface oxygen concentration of the sample as calculated from the Ti2p and O1s core levels is 9.6% and 8.9 at% respectively thus validating the 1:1 stoichiometry assumption. This allows now to estimate the oxygen content related to the N1s surface oxygen component at 396.2 eV by subtracting the amount of surface adsorbed oxygen from the total oxygen content of the surface. It follows that around 4 at% oxygen relate to the N1s surface oxygen component, which corresponds to 5.6 at% nitrogen, and that the N/O ratio is therefore ≈1.4.

To conclude this section, the combined XPS and LEIS data showed that oxygen preferentially interacts with the Ti3d spill-over electrons during chemisorption, which results into selective binding of oxygen to titanium on the surface. Further, self-limited inward migration of oxygen occurs resulting into a stable situation, where some oxygen is dissolved in subsurface layers.

2.2. Oxidation at 5×10^{-2} Pa O_2 and 800 K

The thermal oxidation of TiAlN was studied at an oxygen pressure of 5×10^{-2} Pa and at temperatures of 293 and 800 K. In this set of experiments, performed in a second ultrahigh vacuum (UHV) chamber attached to the XPS chamber, the surface after oxygen chemisorption (1×10^{-5} Pa oxygen for 5 min) served as starting point for enhanced oxidation in order to mitigate adsorption of organic contaminations during transfer. The amount of adventitious carbon was generally below 2 at% and neglected in the following analysis. The corresponding XPS core level spectra are shown in **Figure 3**.

Following oxidation at 293 K for 3 h (Figure 3a), the appearance of a broad Ti2p component centered at 457.4 eV was clearly visible. This component can be, as in the chemisorption case, assigned to surface oxygen. However, since the Ti2p peak for oxynitrides is also expected in the range of 455.5–457.7 eV, we assign this component to a mixture of oxynitridic TiAl(O,N) and surface oxygen.[17] This is supported by the N1s component at 396.2 eV, which was clearly more intense than in the chemisorption experiment and is typical for TiAl(O,N).[17] The joined behavior of Ti2p and N1s peaks was thus interpreted in terms of the inset of enhanced surface oxide growth via an oxynitridic TiAl(O,N) growth region.[2] The O1s peak was decomposed into two components located at 531.8 and 530.3 eV. The precise chemical nature of both components could not be entirely resolved. This is because the components used for the chemisorption of oxygen (Figure 1a) overlap with the oxygen signal

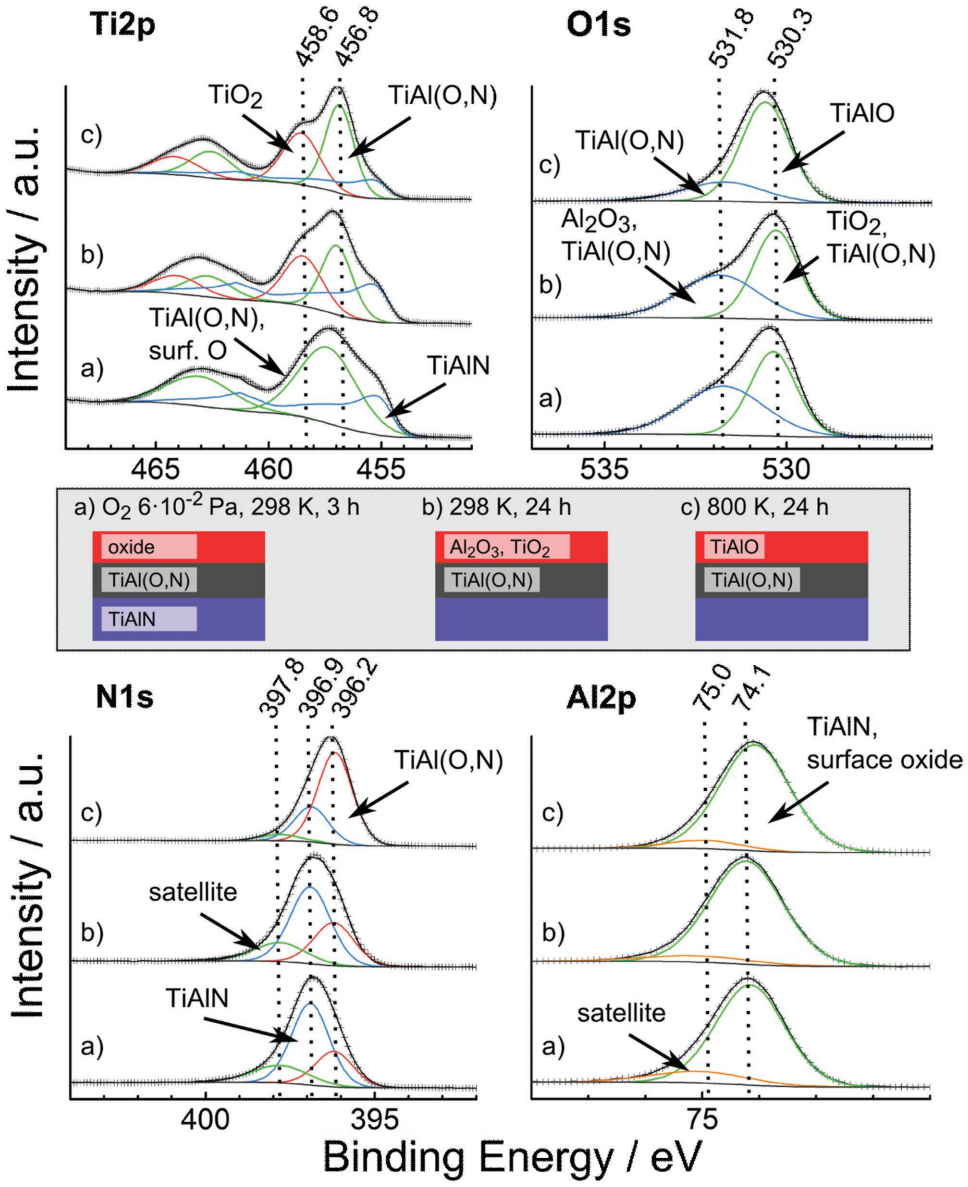

Figure 3. High-resolution XPS spectra of the Ti2p, O1s, N1s, and Al2p core levels of TiAlN after Ar^+ sputtering and a) exposure to 5×10^{-2} Pa O_2 for 3 h at 293 K, b) exposure to 5×10^{-2} Pa O_2 for 24 h at 293 K, and c) exposure to 5×10^{-2} Pa O_2 for 24 h at 800 K. The spectra have been normalized and shifted vertically for better visualization and the raw data are represented by symbols (+). The sketch illustrates the corresponding surface layer model for each experimental condition.

of the TiAl(O,N) growth region. Further, it is shown below that segregation into Al_2O_3 and TiO_2 sets in during oxidation at room temperature, which additionally impedes a precise chemical assignment. The Al2p peak showed as in the chemisorbed case no relevant variation of the lineshape and binding energy with respect to the clean, oxide-free TiAlN surface.

Longer oxygen exposures for 24 h at different substrate temperatures were also investigated. The corresponding XPS spectra are shown in Figure 3b (substrate temperature 273 K) and c (substrate temperature 800 K). The most notable effect in both cases was seen in the Ti2p component, for which two well separated components appear at 456.8 and 458.6 eV. The complete lineshape was described by fixing the shift of the spin-orbit split components to 5.7 eV and the intensities to 0.44 of the related $Ti2p_{3/2}$ components. This intensity value contrasts the expected value of 0.5 but was the experimentally observed ratio when using a Shirley background. The component at 458.6 eV is assigned to Ti in its highest oxidation state, which could correspond to either TiO_2 or to TiAlO and is for the moment simply described as "Ti(IV)."[14] The component at 456.8 eV describes the contribution from TiAl(O,N). The oxynitride component is also clearly identified in the N1s peak at 392.2 eV by its increase in intensity.

The decomposition of the Ti2p into two clearly separated components makes the question arise whether they correspond to phases separated in a multilayer structure. Additional angle

Table 2. Surface layer thicknesses of the different surface oxide layers as obtained after exposure to oxygen at 5×10^{-2} Pa (see the Supporting Information for details of the calculation).

Temperature [K]	Duration [h]	d\{TiAl(O,N)\} [nm]	d\{Ti(IV)\} [nm]
293	3	1.96	–
293	24	1.26	0.66
800	24	2.18	0.75

resolved measurements (see Figure S2, Supporting Information) done in this case showed that the Ti(IV) component was closer to the surface than the TiAl(O,N) component, which indicates the formation of a fully oxidized layer onto a TiAl(O,N) sublayer.

Assuming a clear separation of these two layers, it is possible to use the relative ratios of the Ti2p components to estimate their thickness, which are shown in **Table 2** (see supporting information for details about the calculation). A comparison of the two experiments performed at room temperature and different times shows that after 3 h a TiAl(O,N) layer of about 2 nm thickness is formed. Longer exposure times at the same temperature show that this layer separates with time into a fully oxidized Ti(IV) top layer of about 0.7 nm thickness and an underlying 1.3 nm thick TiAl(O,N) layer. In comparison, oxygen exposure for 24 h at 800 K resulted into a clear increase of the underlying TiAl(O,N) thickness to 2.2 nm, while the Ti(IV) layer at 0.7 nm showed only a negligible increase in thickness with respect to the low temperature case.

Assuming a model of perfectly separated layers, the observed behavior can be explained as a stepwise formation of first a TiAl(O,N) growth region due to inward migration of oxygen and then the establishment of a top layer of fully oxidized Ti(IV). This interpretation is also supported by recent investigation on the electrochemical oxidation of TiAlN, where the electrochemical oxidation of TiAlN could be described by a reactive migration mechanism as well.[29] The relevance of the oxygen inward migration for the oxidation is further highlighted by the Al/Ti ratios reported in Table 1: though preponderant aluminum outward migration is expected in the case of the high temperature TiAlN oxidation, the Al/Ti ratios remained rather constant and only slight enrichment of aluminum was observed at 800 K.[2]

Additional information about the nature of this rather generically described Ti(IV) layer can be obtained by a careful analysis of the O1s peak after the exposure for 24 h. In Figure 3, the O1s peaks were decomposed into two components: after oxidation at room temperature (case b) the binding energies and relative ratios of these components were 530.2 (54%) and 531.7 eV (46%) and after oxidation at 800 K (case c) the binding energies and relative ratios were 530.3 (76%) and 531.4 eV (24%). In both cases, the lower binding energy position component at about 530.3 eV can be assigned to either mixed TiAlO (see film 3 of Cremer et al.[30]) or TiO_2.[3,17,27,31] The other component at 531.7 eV could relate to oxynitride or Al_2O_3 according to its binding energy.[3,32–34] In this regards, it must be noted that the partial pressure of water during the long-term 24 h oxidations was 1.2×10^{-6} Pa due to the purity of the gas and was thus not negligible. The presence of water might eventually result into hydroxylation, and could easily account for the higher binding energy components.[35–37] However, the angle-resolved O1s spectra shown in Figure S2 (Supporting Information) show surface depletion of the higher binding energy components, which allows to exclude the presence of surface hydroxylation or the adsorption of water.

The question is now open whether the topmost layer is composed by a segregated two-phase mixture of TiO_2 and Al_2O_3 or by a homogenous TiAlO layer. This problem was addressed by an analysis of the O1s modified Auger parameter of the samples. The corresponding Wagner plot is shown in **Figure 4**.

It was found that the modified Auger parameter dropped after oxidation at 800 K, whereas at 293 K only a small decrease was observed. Since the modified Auger parameter is a measure for the extra-atomic relaxation energy of the core hole, this indicates a decrease of the polarizability of surface oxides, which depends on the temperature of oxidation.[38,39] In this regard, it is noted that due to the small depth of information the modified Auger parameter dominantly reflects the polarizability of the so-called Ti(IV) outer layer. This allows for a comparison with values for metastable mixed TiAlO, which was earlier investigated by Cremer et al., who identified two separated regimes that were ascribed to segregated Al_2O_3 and TiO_2 at 1042 eV and mixed TiAlO between 1037 and 1041 eV.[30] In our case, the Auger parameter of the surface oxide formed at 293 K indicates the inset of segregation, whereas at 800 K a mixed TiAlO apparently grows.

These results can be corroborated by cross-peak self-consistent stoichiometric calculations.[28] Following these principles, the oxygen concentrations related to TiO_2 and TiAlO formed after 24 h at 293 and 800 K were calculated from the

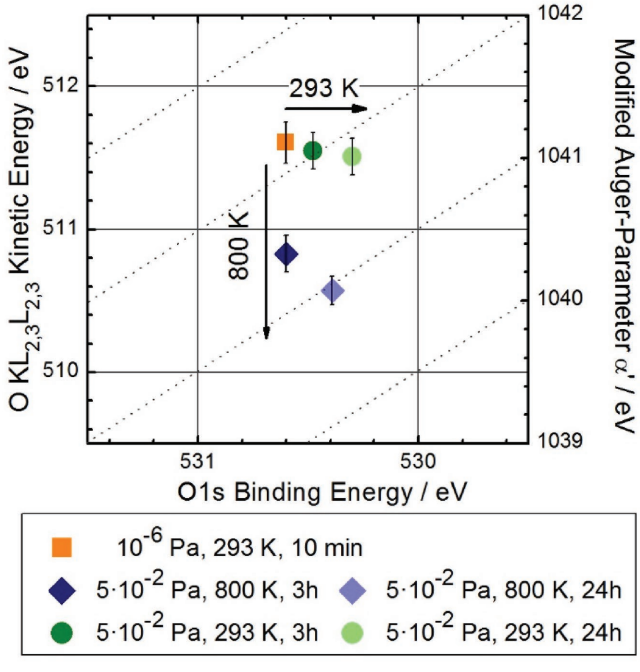

Figure 4. Wagner plot of the O1s modified Auger parameter of the surface oxide layer formed on the samples investigated in this work. The uncertainty of the O1s binding energy was below 65 meV.

Table 3. Cross-peak self-consistent calculations of the assignments of the Ti(IV) component of the Ti2p and O1s peaks in the case of oxidation for 24 h at 293 and 800 K based on the sample stoichiometries from Table 1.

Temperature [K]	Transition	Components BE [eV]	Proposed assignment	X_o [at%]
293	Ti2p	468.6	TiO_2	10.7
	O1s	530.2	TiO_2	14.7
		531.7	Al_2O_3	12.5
800	Ti2p	468.6	TiAlO	25.7[a)]
	O1s	530.3	TiAlO	23.8
		531.4	TiAl(O,N)	10.7

[a)]The concentration of oxygen bound to Al(III) in TiAlO was calculated by assuming that the Al2p component associated with TiAlO (not resolved in the Al2p peak) had the same fraction as that of the corresponding Ti2p component.

respective Ti2p and O1s components. The results are shown in **Table 3**. For the oxidation at 800 K it was assumed that the fraction of Al2p related to TiAlO is the same as for Ti2p, because the Al2p lineshape was unaffected by oxidation and no TiAlO-related Al2p component could be resolved. With this assumption, the surface oxygen concentration due to TiAlO is either 25.7 or 23.8 at% when calculated from either the O1s or the Ti2p spectra. Since these values are essentially identical, the assignments of the TiAlO components in the O1s and Ti2p spectra are in mutual agreement and thereby corroborated. Further, the calculation shows that the lower binding energy O1s component at 531.4 eV corresponds to TiAl(O,N) in the case of oxidation at 800 K.

After oxidation at 293 K no spectral components could be assigned unambiguously due to uncertainties of the peak position of the TiAl(O,N) component, which depends on the oxidation temperature.[28]

In conclusion, Wagner plot analysis in combination with cross-peak self-consistent calculations indicates that the oxidation at 800 K results into mixed TiAlO whereas at 293 K segregation into Al_2O_3 and TiO_2 occurs. An illustration of this surface layer model is shown in **Figure 5**

2.3. Electronic Properties of the Surface Near Regions

A more thorough characterization of the electronic properties of the surface oxides during the different stages of oxidation was done by Ultraviolet Photoelectron Spectroscopy (UPS) measurements of the valence band region. The results for the sample oxidized at 800 K during 24 h are shown in **Figure 6** and are representative for the oxidation at both temperatures (see Figure S3 (Supporting Information) for the spectra of the sample oxidized at 293 K).

Following Ar^+ sputter cleaning (Figure 6a), a Fermi cutoff was observed and attributed to Ti3d electrons present at 0 eV binding energy, which reflects the metallic behavior of the hard coating. The broad band around 5 eV is ascribed to mixed N2p/Al3p states (p-band).[15] After chemisorption of oxygen (Figure 6b) a decrease of the Ti3d electron density and relative increase of the p-band intensity was observed. This is explained by the capture of Ti3d electrons by oxygen and the incorporation of O2p states into the p-band.[26] The fact that Ti3d states are still present at the Fermi level shows that the near-surface region is not completely oxidized and that the oxygen incorporation does not reduce the metallic character significantly in the chemisorbed case. By contrast, the Ti3d component disappeared in the thermally oxidized case (Figure 6c).

The quasi-metallic character of the oxygen chemisorption layer was also reflected by the corresponding Ti2p spectrum in Figure 1b, where only surface oxygen but not the subsurface oxygen affected the Ti2p lineshape. Considering that strong interactions between O2p and Ti3d states occur, it is supposed that the oxygen concentrations in buried layers are diluted. This interpretation is in accordance with the initial stages of the oxidation of α_2-TiAl, where similarly adsorption and incorporation of oxygen into the metallic alloy was observed.[27]

Apart from the decrease of intensity at the Fermi level, another effect of the progressive incorporation of oxygen into the surface is the appearance of a shoulder at about 3 eV during chemisorption that shifts toward an approximate position of 2 eV after thermal oxidation. Based on the partial density of states of TiAl(O,N) we attribute this shift to changes in the p-band: preferential binding of oxygen to aluminum substitutes the nitrogen–aluminum bonds and pushes the N2p band to lower binding energies.[26] The nitrogen can thus be regarded to act essentially as a deep trap. This explanation is corroborated by nitrogen doping studies of TiO_2, where a similar electronic structure is observed and nitrogen dopants present on lattice sites are also forming the oxynitridic O–Ti–N structure with a similar N1s binding energy of 397 eV.[40,41] Considering further the low depth of information of UPS, this further implicates that the oxidized top layers formed after oxidation are nitrogen-doped.

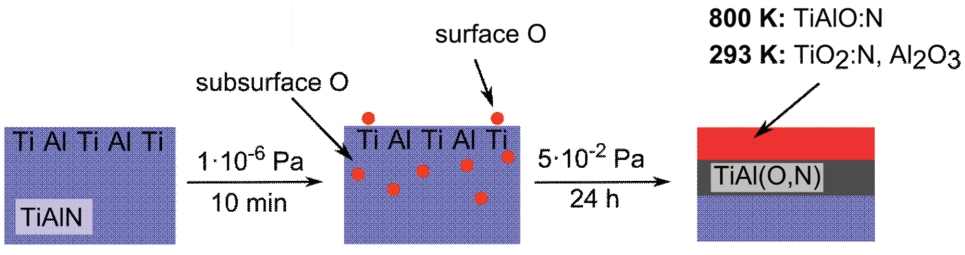

Figure 5. Schematic of different stages of surface oxide growth on TiAlN assuming a model of sharp separation between layers. Note that the illustration is not at scale.

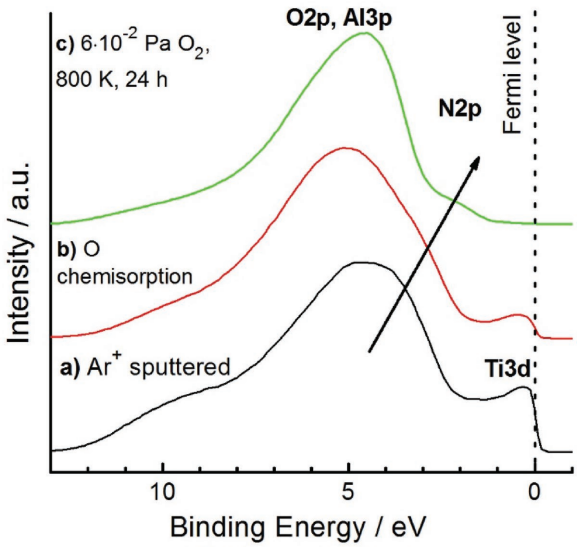

Figure 6. UPS (21.2 eV) valence band measurement of TiAlN after a) Ar^+ sputter cleaning, b) chemisorption at $p(O_2) = 1 \times 10^{-6}$ Pa and 293 K for 10 min, c) oxidation at $p(O_2) = 5 \times 10^{-2}$ Pa and 800 K for 24 h. The spectra were normalized and shifted vertically for better visualization.

3. Conclusion

The transition from oxygen chemisorption to surface oxidation of TiAlN was investigated by means XPS, UPS, and LEIS. The results show that the nonoxidized Ar^+ sputter cleaned surface is essentially metallic, and terminated by titanium and aluminum. Subsequent oxygen chemisorption at 5×10^{-6} Pa leads to selective binding of oxygen to titanium sites and a concomitant inward migration of oxygen. This process does not result into a 3D surface oxide, but is restricted to the incorporation of oxygen without substantially changing the metallic character of the subsurface layers.

During oxidation at oxygen partial pressure of 5×10^{-2} Pa, a multilayered surface oxide formed on top of an oxynitridic growth region due to reactive inward migration of oxygen. The nitrogen within that region was found to be destabilized due to reactive exchange of Al—N bonds by Al—O bonds. The structure of the formed surface oxides was determined by the temperature: detailed chemical analysis using the Wagner plot indicated the formation of a mixed TiAlO top layer at 800 K, whereas the oxide segregated at 293 K into TiO_2 and Al_2O_3. These results are of high relevance for postprocessing of TiAlN directly after deposition and its reactivity in contact with polymer melts.

4. Experimental Section

Thin Film Deposition: The HPPMS deposition process was chosen due to the superior quality of the coatings. As described elsewhere, TiAlN thin films with a thickness of 1.2 µm were deposited on boron-doped (100) Si wafer (1–5 Ω cm).[29] The deposition chamber (CemeCon CC-800/9) was equipped with a rectangular magnetron (500×88 mm^2) and a Ti/Al compound target, which provided a Ti/Al ratio of nearly 1 and was located 80 mm away from the substrates. The substrates were held at floating potential and heated to 550 K. Sputter deposition was performed at 800 Hz with an on-time of 50 µs, which gives a time-averaged power density of 6.8 W cm^{-2} and a peak power density of 0.4 kW cm^{-2}. The gas pressure inside the chamber was 0.46 Pa and the Ar:N_2 ratio was set to 4:1. The structure of the samples was characterized by X-Ray Diffraction and a random structure was found.[29] The density of the TiAlN was around 4.8 g cm^{-3} and the stoichiometry was $Ti_{0.2}Al_{0.3}N_{0.5}$ as determined by an Ar^+ sputtered sample measured by XPS. Minor bulk oxygen contaminations were also found by XPS and are neglected in the following discussion (2.4 at%).

Sample Preparation: The as-deposited samples were sonicated in analytical grade ethanol for 5 min before introduction into the UHV environment of the characterization chamber. In situ cleaning of the specimens was performed by Ar^+ sputtering using the Figure 5 from PHI Physical Instruments (3 kV, 8 µA cm^{-2}, 20 min, 30° angle of incidence) until the residual O content of the near-surface layer decreased to a constant value below 2.5 at% as determined by XPS. After this cleaning step the samples were exposed to different oxygen pressures (99.998%, <2 ppm H_2O, Air Liquide) at different substrate temperatures and exposure times. The room temperature (293 K)-low pressure (1×10^{-6} Pa) experiments were performed directly in the analytical chamber of the XPS. Enhanced oxidation at 800 or 293 K and higher oxygen pressures (1×10^{-6} and 5×10^{-2} Pa) was performed in a second UHV-preparation chamber directly attached to the XPS, so that the samples were transferred between the different chambers without breaking the vacuum.

Surface Chemical Analysis: The UHV facility is composed of two interconnected chambers, one for oxidation experiments, and a second one dedicated to sample characterization by XPS, UPS, and LEIS. The spectrometer was an ESCA+ system (Oxford Instruments, Omicron Nanotechnology). For XPS, monochromated Al Kα irradiation (1486.7 eV) was used, with a source to analyzer angle of 102°. The spectral resolution was 0.77 eV as determined from the silver metal $Ag3d_{5/2}$ lineshape. Similarly, the binding energy was referenced to the $Ag3d_{5/2}$ line at 368.0 eV and no charge neutralizer was used. Unless otherwise stated, XPS spectra were measured at an emission angle of 15° relative to the surface normal, resulting into an information depth of the measured core level spectra (O1s, Ti2p, N1s, Al2p) of ≈5.5 nm.[42] For the construction of Wagner plots the X-ray excited O KLL spectra were measured at 15°, while the O1s spectra were taken at 60°. This was done in order to match a similar value of the information depth of 2.7 nm, taking into account the different attenuation lengths of the emitted electrons due to their different kinetic energies.[42] The modified Auger parameter was then calculated by adding the value of the O1s binding energy to the kinetic energy of the oxygen KLL signal.[39] The acquired XPS data were evaluated with CasaXPS (2.3.15 Casa Software Ltd.) using asymmetry corrected elemental sensitivity factors and GL(30) lineshapes. Peak fitting was performed without any constraints and using a Shirley background unless otherwise stated. A Monte Carlo procedure for estimating uncertainties of fit parameters was used as implemented in CasaXPS. Generally, the uncertainty of XPS components was better than 0.07 eV and is thereby neglected. The error of the oxygen KLL signals for the construction of the Wagner plots was estimated by empirically fitting the KLL peak by three GL(30) peaks and making similarly use of the Monte Carlo method. The HeI line at 21.2 eV was used for UPS measurements (HIS 13 VUV Source, Omicron Nanotechnology). The geometry of the He^+ LEIS comprised an incidence angle and an emission angle of 30° and 60° with respect to the surface normal resulting into a scattering angle of 115°. The flux of the primary He^+-ions generated by the Figure 5 sputter gun with an energy of 1 kV was $\approx 1 \times 10^{13}$ ions cm^{-2} s^{-1} and can be thus regarded as destructive.[25] The beam was rastered across an area of 1 mm^2 in order to increase the sensitivity. The acquisition time of a single spectrum was 75 s with an energy resolution of 2.2 eV.

Supporting Information

Supporting Information is available from the Wiley Online Library or from the author.

Acknowledgements

The authors gratefully thank M. to Baben and J. M. Schneider for the synthesis of the hard coating. Further, the authors acknowledge the German Research Foundation (DFG) for financial support within the Transregional Collaborative Research Center SFB TR 87.

Received: September 6, 2016
Revised: October 20, 2016
Published online: December 19, 2016

[1] T. Leyendecker, O. Lemmer, S. Esser, J. Ebberink, *Surf. Coat. Technol.* **1991**, *48*, 175.
[2] S. Hofmann, *Thin Solid Films* **1990**, *193–194*, 648.
[3] F. Esaka, K. Furuya, H. Shimada, M. Imamura, N. Matsubayashi, T. Kikuchi, H. Ichimura, A. Kawana, *Surf. Interface Anal.* **1999**, *27*, 1098.
[4] J.-L. Huang, B.-Y. Shew, *J. Am. Ceram. Soc.* **1999**, *82*, 696.
[5] K. Bobzin, R. Nickel, N. Bagcivan, F. D. Manz, *Plasma Process. Polym.* **2007**, *4*, S144.
[6] V. Kouznetsov, K. Macák, J. M. Schneider, U. Helmersson, I. Petrov, *Surf. Coat. Technol.* **1999**, *122*, 290.
[7] K. Sarakinos, J. Alami, S. Konstantinidis, *Surf. Coat. Technol.* **2010**, *204*, 1661.
[8] D. Lundin, K. Sarakinos, *J. Mater. Res.* **2012**, *27*, 780.
[9] J. T. Gudmundsson, N. Brenning, D. Lundin, U. Helmersson, *J. Vac. Sci. Technol., A* **2012**, *30*, 030801.
[10] D. Music, J. M. Schneider, *New J. Phys.* **2013**, *15*, 073004.
[11] G. Greczynski, S. Mráz, L. Hultman, J. M. Schneider, *Appl. Phys. Lett.* **2016**, *108*, 041603.
[12] C. Kunze, D. Music, M. to Baben, J. M. Schneider, G. Grundmeier, *Appl. Surf. Sci.* **2014**, *290*, 504.
[13] S. Hofmann, *Philos. Trans. R. Soc., A* **2004**, *362*, 55.
[14] *NIST X-Ray Photoelectron Spectroscopy Database*; Version 4.1, National Institute of Standards and Technology, Gaithersburg, MD **2012**.
[15] I. leR. Strydom, S. Hofmann, *Vacuum* **1990**, *41*, 1619.
[16] L. Porte, L. Roux, J. Hanus, *Phys. Rev. B* **1983**, *28*, 3214.
[17] P. Prieto, R. E. Kirby, *J. Vac. Sci. Technol., A* **1995**, *13*, 2819.
[18] A. Arranz, C. Palacio, *Surf. Sci.* **2006**, *600*, 2510.
[19] G. Greczynski, J. Jensen, J. E. Greene, I. Petrov, L. Hultman, *Surf. Sci. Spectra* **2014**, *21*, 35.
[20] A. Schüler, P. Oelhafen, *Phys. Rev. B* **2001**, *63*, 115413.
[21] A. J. Perry, *J. Vac. Sci. Technol., A* **1988**, *6*, 2140.
[22] D. Jaeger, J. Patscheider, *J. Electron Spectrosc. Relat. Phenom.* **2012**, *185*, 523.
[23] I. Milošv, H.-H. Strehblow, B. Navinšek, M. Metikoš-Huković, *Surf. Interface Anal.* **1995**, *23*, 529.
[24] Z. Zhang, Y. Nie, L. Shen, J. Chai, J. Pan, L. M. Wong, M. B. Sullivan, H. Jin, S. J. Wang, *J. Phys. Chem. C* **2013**, *117*, 11656.
[25] H. H. Brongersma, M. Draxler, M. de Ridder, P. Bauer, *Surf. Sci. Rep.* **2007**, *62*, 63.
[26] M. to Baben, L. Raumann, J. M. Schneider, *J. Phys. Appl. Phys.* **2013**, *46*, 084002.
[27] V. Maurice, G. Despert, S. Zanna, P. Josso, M.-P. Bacos, P. Marcus, *Acta Mater.* **2007**, *55*, 3315.
[28] G. Greczynski, L. Hultman, *Appl. Surf. Sci.* **2016**, *387*, 294.
[29] M. Wiesing, M. to Baben, J. M. Schneider, T. de los Arcos, G. Grundmeier, *Electrochim. Acta* **2016**, *208*, 120.
[30] R. Cremer, M. Witthaut, D. Neuschütz, *Fresenius' J. Anal. Chem.* **1999**, *365*, 28.
[31] I. Bertóti, M. Mohai, J. L. Sullivan, S. O. Saied, *Appl. Surf. Sci.* **1995**, *84*, 357.
[32] H. C. Barshilia, N. Selvakumar, K. S. Rajam, D. V. Sridhara Rao, K. Muraleedharan, *Thin Solid Films* **2008**, *516*, 6071.
[33] V. Maurice, H.-H. Strehblow, P. Marcus, *Surf. Sci.* **2000**, *458*, 185.
[34] L. P. H. Jeurgens, W. G. Sloof, F. D. Tichelaar, E. J. Mittemeijer, *Surf. Sci.* **2002**, *506*, 313.
[35] E. McCafferty, J. P. Wightman, *Surf. Interface Anal.* **1998**, *26*, 549.
[36] G. Ketteler, S. Yamamoto, H. Bluhm, K. Andersson, D. E. Starr, D. F. Ogletree, H. Ogasawara, A. Nilsson, M. Salmeron, *J. Phys. Chem. C* **2007**, *111*, 8278.
[37] X. Deng, T. Herranz, C. Weis, H. Bluhm, M. Salmeron, *J. Phys. Chem. C* **2008**, *112*, 9668.
[38] C. D. Wagner, *Faraday Discuss. Chem. Soc.* **1975**, *60*, 291.
[39] G. Moretti, *Surf. Sci.* **2013**, *618*, 3.
[40] C. Gnoth, C. Kunze, M. Hans, M. to Baben, J. Emmerlich, J. M. Schneider, G. Grundmeier, *J. Phys. Appl. Phys.* **2013**, *46*, 084003.
[41] C. Di Valentin, A. Tilocca, A. Selloni, T. J. Beck, A. Klust, M. Batzill, Y. Losovyj, U. Diebold, *J. Am. Chem. Soc.* **2005**, *127*, 9895.
[42] C. Di Valentin, G. Pacchioni, A. Selloni, *J. Phys. Chem. C* **2009**, *113*, 20543.

